

EXPERIMENTAL BEAM DYNAMICS IN THE SLC LINAC*

J. T. SEEMAN, I. E. CAMPISI, W. HERRMANNSFELDT, M. LEE, A. PETERSEN AND D. TSANG
Stanford Linear Accelerator Center, Stanford University, Stanford, California 94305

G. S. ABRAMS

Lawrence Berkeley Laboratory, Berkeley, California 94720

C. ADOLPHSEN

University of California, Santa Cruz, California 95064

and

E. SODERSTROM

California Institute of Technology Pasadena, California 91125

1. Abstract

The component installation for the upgrade of the three-kilometer linac¹ for the SLAC Linear Collider (SLC) was completed in late summer 1986. The system status and measurements of beam properties made during commissioning are described in this paper. Further linac measurements are reviewed in companion papers.^{2,3,4}

In summary, a low-emittance electron beam from a damping ring has been accelerated through the linac and injected into the north SLC Arc with negligible loss. The maximum bunch intensity is 2.9×10^{10} electrons/pulse. A peak particle energy of 53 GeV has been reached. Operation at 47 GeV is now routine. The energy and energy spectrum of the electron beam can be rapidly measured nondestructively at high energy. These signals will be used in a fast feedback system nearing completion. The electron beam can be centered in the accelerator to about 200 μm rms. Slow feedback of the injection position and angle into the linac and injection into the north Arc are operational.⁵ Longitudinal and transverse wakefields have been measured and appear to be near expectations. Transverse position measurements at the end of the linac show a 120 μm horizontal and a 30 μm vertical (rms) jitter from pulse to pulse. The spot shape, including the transverse tails, also shows some jitter. The transverse position and shape fluctuations have several sources involving launch instabilities, chromatic effects, RF deflections and lattice mismatches. Continued improvements are expected. These parameter jitters would not preclude collisions. The measured invariant transverse emittances of the beam at 47 GeV are 2×10^{-5} m^2 vertically and $12 - 25 \times 10^{-5}$ m^2 horizontally at 1×10^{10} e^- . The horizontal emittance increases with beam intensity. Damped positrons have been injected into the linac, and trajectory correction is underway.

Linac Lattice

The quadrupole lattice in the SLC Linac is a FODO array used to maintain the small transverse beam dimensions and to control wakefield emittance growth downstream of the injection point from the damping rings. The horizontal and vertical betatron functions along the linac are shown in Fig. 1. They are calculated by an online computer program and are derived using a matched beam from the damping ring tracked through the linac. The quadrupole spacing is 3 m in the first 100 m of linac, 6 m in the next 200 m, and 12.2 m in the remaining 2645 m. The required spaces for the quadrupoles early in the linac were made possible by removing 5 cells from each of 36 ten-foot accelerating sections and rebrazing. This *beta reduction* project reduced the effect of transverse wakefields by a factor of two. The reduction is due to naturally smaller trajectory deviations in the accelerating structure which reduces the generated wakefields and the increased angular size of the beam which mitigates the effect of a given wakefield.

The 50-GeV design lattice has a 90° phase shift per cell maintained for the first 1500 m. Thereafter, the quadrupoles reach their saturated strengths (106 kG gradient length), and the betatron functions increase slowly leading to a phase shift per cell of 45° at the end of the machine. Lattices with reduced phase

*Work supported in part by Department of Energy, contracts DE-AC03-76SF00515, DE-AC03-76SF00098, DE-AA03-76SF00010 and DE-AC03-81ER40050.

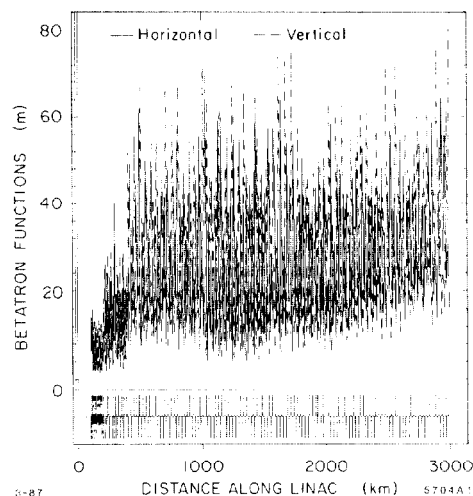


Fig. 1. Linac horizontal and vertical betatron functions. The bottom scale shows the location and polarity of the quadrupoles.

shift per cell can easily be implemented. The spikes in the betatron functions in Fig. 1 arise from an asymmetry in the lattice caused by a 3 m drift section occurring every 100 m. Nearby quadrupoles have been adjusted in the design lattice to minimize the spikes. The lattice now operates at 47 GeV with the design strengths.

A *klystron management* program has been tested which scales the quadrupole strengths throughout the linac in proportion to the beam energy. Thus, when a klystron is removed from the beam and another one is activated, the program keeps the beam energy and the orientation of the phase space ellipse at the end of the linac fixed. This program works well, but minor operational problems with scaling have been encountered when the quadrupole strengths are near their limits.

Trajectory Correction

The trajectories of positrons and electrons are measured in strip line beam position monitors (BPM) mounted inside each quadrupole. The centers of each BPM were electrically measured with a resolution of about 10 microns. Offsets greater than 100 μm were mechanically fixed. The BPM's were centered inside the quadrupoles to within 50 μm . The readout electronics modules were calibrated to 50 μm . The BPM pulse cables were matched and calibrated. The trajectories of the two beams are corrected using a pair of dipole magnets located near each quadrupole. The dipoles have maximum strengths which can compensate for 0.5 to 1 mm quadrupole displacements.

Several trajectory correction algorithms have been tried. Experience with electrons has shown that the so-called one-to-one steering method⁶ works best given the constraints of finite strength correctors, uncertainties in betatron phase shifts and missing correctors or BPM readings. The one-to-one method uses one corrector to center the beam position in the next downstream BPM, as will be explained later. The effects of that corrector on downstream BPM readings are removed before calculating the strength of the next corrector. This method successfully eliminates betatron oscillations. These oscillations cause the bulk of our problems and originate from component

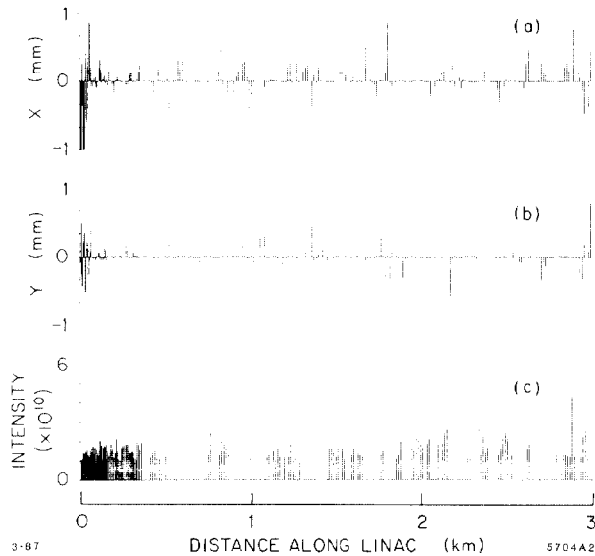


Fig. 2. Measured electron trajectory after correction. Panels a and b are the x and y displacements, respectively. The beam intensity signal is shown in panel c.

variations in the damping rings and the Ring-To-Linac (RTL) transport line (mostly horizontal). The algorithm has worked above $2 \times 10^{10} e^-$ where transverse wakefield effects can substantially distort the position data. The algorithm works methodically down the linac decreasing the orbit deviation as it goes. In the software the linac is divided into three 1 km pieces and is automatically steered in two to three iterations each. This division is necessary because the measured and calculated betatron phase advances remain in-phase only over about 1 km. The entire correction process presently takes 15 minutes. Work to reduce the time to a few minutes is in progress. In Fig. 2 are shown the horizontal (x) and vertical (y) trajectories of a single position measurement in the linac after computer automated steering. The large offsets near the beginning are measurements in the RTL. The displacements near 2 km are due to stray fields of the extraction septum ahead of the positron source. The trajectories near the end of the linac were left uncorrected to show betatron oscillations in both x and y . The rms trajectory error is about $200 \mu\text{m}$ for both x and y .

When all dipoles and position monitors were used in the correction algorithm, many of the dipole correctors were required to be near or above their maximum strengths. The cause was that the offset errors in the BPM's located in the defocussing quadrupoles required effectively much larger dipole strengths to compensate them than in the focussing quadrupoles. When only the dipoles and BPM's at focussing quadrupoles were used, the net dipole strengths were reduced by a factor of four allowing an easier correction. Because of the varying betatron function in a FODO lattice, a beam is expected to be closer to the accelerator axis in the defocussing quadrupole than the focussing ones and need not be corrected there. Furthermore, the transverse wakefields are larger at the focussing quadrupoles where the betatron function and trajectory errors are maximum. It is there that correction is most effective. The correction of the positron beam will use the dipoles and BPM's in their focussing quadrupoles which are complementary to those for the electrons. The shared magnets will cause some correction coupling between electrons and positrons, but because of the out-of-phase betatron functions, there is a decoupling of about a factor of 4. The electron trajectory in Fig. 2 was corrected at only the electron focussing magnets. The corrected BPM's have readings of order 10 to $30 \mu\text{m}$. What remains and dominates in the figure are the position readings in the *unused* BPM's. Thus, an upper limit of the BPM errors can be set at less than $200 \mu\text{m}$. The unused correction dipoles have been set to zero strength until positrons are steered in the linac.

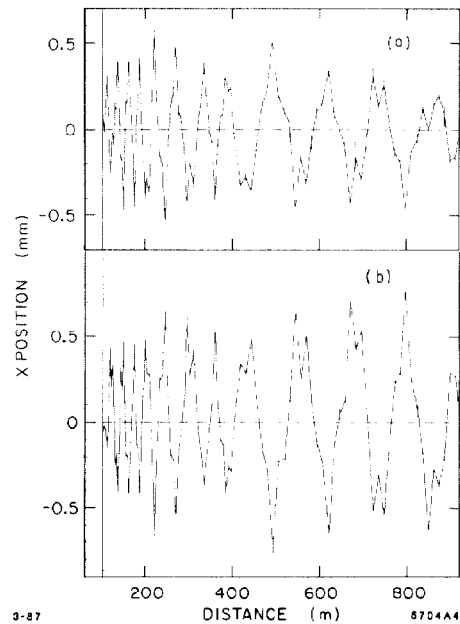


Fig. 3. Measured trajectories of an accelerated electron beam due to a 3 Gm dipole deflection: (a) low intensity (8×10^9) and (b) high intensity (2.2×10^{10}). Note the trajectory differences downstream caused by transverse wakefields.

Trajectory Changes from Transverse Wakefields

A bunch executing a betatron oscillation in the linac will be subject to transverse wakefield effects. These effects have been seen quite clearly on profile measurements of the beam at the end of the linac as non-Gaussian transverse tails. These tails can be digitized and studied. (See Ref. 3.) The centroid positions of the bunch along the linac are also changed by these asymmetric tails and can be detected in the position monitors.

The betatron oscillations of a bunch at two different intensities are shown in Fig. 3. In the measurements which are averages over several BPM readings, a nominal trajectory was recorded after steering correction. A dipole corrector twelve meters from the beginning of the linac was then changed by 3 G meters. The subsequent trajectory was measured and subtracted from the nominal trajectory. This "difference" orbit is shown in Fig. 3a for $8 \times 10^9 e^-$. Another one is shown in Fig. 3b for $2.2 \times 10^{10} e^-$. Note that the initial trajectories for the two tests are very similar but begin to deviate from each other more and more after 200 m. This difference is direct evidence of transverse wakefields. This conclusion has been corroborated using a simulation program, WAKTRK. This program uses four longitudinal slices per millimeter and the transverse and longitudinal wakefields of the SLAC structure and the actual energy gain profile and quadrupole lattice of the SLC. The overall RF phase is always adjusted to maintain the narrowest energy spectrum at 47 GeV. Simulations of the average beam position in the linac were made at low and high beam currents with conditions matching those of the experimental data in Fig. 3. The results are shown in Fig. 4. The simulations and the data agree remarkably well. There is a difference in the amplitudes of the beam positions at high current between the simulations and measurements of about 40%. This is attributed to uncertainties in the initial energy spread and in the longitudinal density distributions, due to bunch lengthening in the damping rings and the ensuing nonlinear compression and aperture clipping in the RTL. Fortunately, the experimentally observed wakefield effects appear to be smaller than the simulations predict.

Long-Range Transverse Wakefield Effects

The SLC must operate with three bunches in the linac with an interspacing of approximately 60 nsec. To test for the possible effects of long range transverse wakefields, two bunches from the CID injector⁷ were accelerated down the linac to 42 GeV.

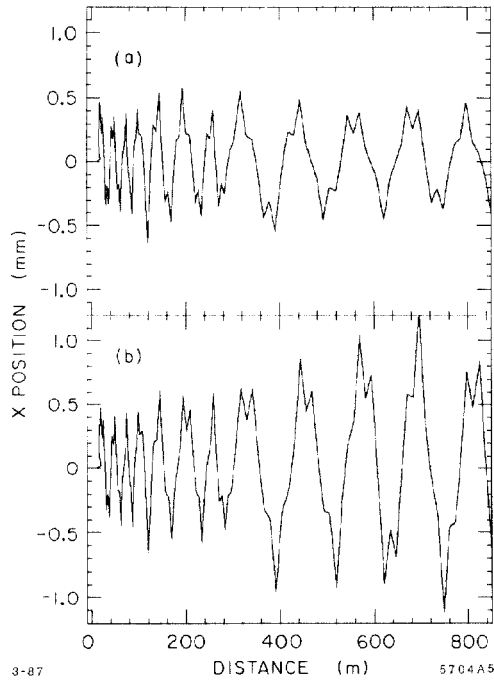


Fig. 4. Simulated trajectories of an accelerated electron beam with conditions of Fig. 3. The simulations (a) and (b) used $\sigma_x = 1$ mm at 8×10^9 and 2.5 mm at 2.2×10^{10} , respectively.

The bunches from CID have a transverse emittance about ten times that of the SLC damping ring and a longitudinal charge distribution of approximately two millimeters (rms). The first bunch had a charge of $6 \times 10^9 e^-$ and the second $2 \times 10^9 e^-$. The trajectories of both bunches were within $500 \mu\text{m}$ rms of the accelerator axis after the first bunch's trajectory was corrected. An upstream dipole magnet was then energized causing a betatron oscillation in both bunches of 6 mm. The resulting trajectories of the second bunch with and without the first bunch present are shown in Fig. 5. If significant long-range transverse effects were present, the trajectory differences should be much larger. The small differences are consistent with chromatic effects from energy changes due to beam loading, about 100 MeV.

Transverse Beam Profiles

The beam profile must be observed at the end of the linac to control transverse wakefields³, to match the phase space orientation to the Arc lattice and to measure the beam emittance. The beam size is measured using a fluorescent screen monitor⁸

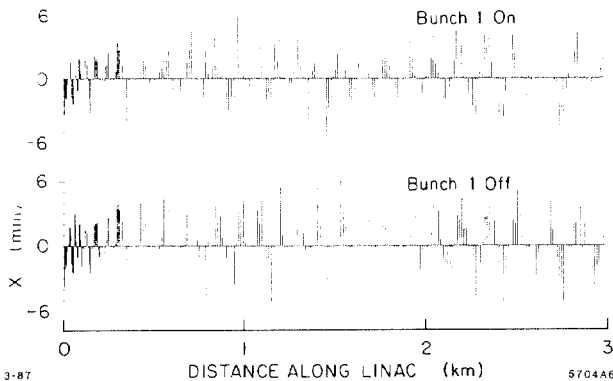


Fig. 5. Measured horizontal trajectories for a 2×10^9 electron bunch. (a) is with a leading 6×10^9 electron bunch 60 nsec ahead and (b) without the leading bunch. This experiment tested for long range transverse wakefields effects.



Fig. 6. Profile of a 47-GeV , 2×10^{10} electron bunch. The fiducial holes are separated 3 mm horizontally and 1 mm vertically.

and a diode array TV camera. A typical profile of a beam is shown in Fig. 6, observed just before the splitter magnet at the beginning of the Arc. The core of the beam contains about 90% of the 2.2×10^{10} electrons and has a crescent shape due to launch conditions from the RTL and also due to dispersive effects from the bunch's large energy spread (1 to 2%). The long tail is mostly in the horizontal plane and arises from a tail on the beam present at the linac entrance and from transverse wakefield effects. Dipole steering early in the linac can remove the wakefield induced tails. At higher intensities ($> 1.5 \times 10^{10} e^-$) the bunch length becomes quite long (> 2 mm) and dispersive (chromatic) effects contribute significantly to the transverse shape. Nevertheless, minor adjustments of the launch steering and overall RF phase lead to a Gaussian beam core suitable for emittance and phase space measurements. A beam spot which has been digitized from the TV video output is shown in Fig. 7c and projected onto the x and y axes in Fig. 7a and b. The smallest measured spot width of $37 \mu\text{m}$ sigma is very near the design resolution of the screen/TV system. Simultaneous x and y beam widths of $157 \mu\text{m}$ and $99 \mu\text{m}$, respectively, have been measured at 47 GeV and $8 \times 10^9 e^-$. This meets the design specifications. The spot shape can be measured as a function of quadrupole strength and the emittance and the lattice parameters (β , α) can be estimated from the measurement. A sample data set is

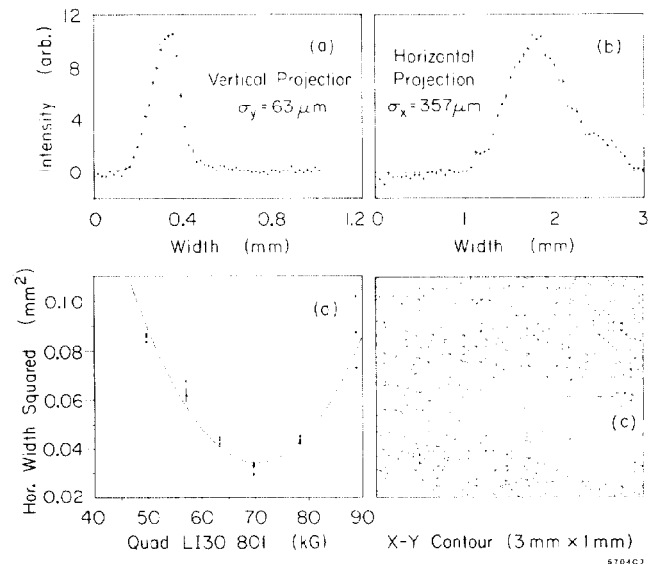


Fig. 7. Digitized beam profile and emittance measurements at 47 GeV. (a) is a vertical projection, (b) a horizontal projection, (c) an intensity contour, and (d) a display of beam width versus quadrupole strength.

Table I

Summary of Transverse Emittance Measurements. Invariant emittance $\gamma\epsilon$ is in units of 1×10^{-5} rm. The beam current I is in units of 1×10^{10} and the beam energy E in GeV.

Location in Linac	I	E	$\gamma\epsilon_x$	$\gamma\epsilon_y$
Ring Exit	2	1.2	2.2 ± 0.3	0.4 ± 0.1
0 Km	2	1.2	13 ± 3	1.3 ± 0.3
1 Km	0.7	8.5	8 ± 1	
1 Km	1.5	8.5	11 ± 2	2.5 ± 0.3
3 Km	0.4	43	7 ± 1	
3 Km	0.8	47	12 ± 4	1.1 ± 0.3
3 Km	1.0	34	25 ± 5	2.1 ± 1.0
3 Km	1.5	43	20 ± 5	4 ± 1

shown in Fig. 7d for a $2.2 \times 10^{10} e^-$ beam. The derived lattice functions are within a factor of two of the design values and will be corrected. Seven independently adjustable quadrupoles near the end of the linac will be used to match the beam to the Arc. A summary of emittance measurements is shown in Table I. The beam emittance enters the linac somewhat enlarged, and at low intensities does not become larger in the linac. But, at high intensities the horizontal emittance is significantly larger. This increase is directly linked to enlarged energy spectra, wakefield and chromatic effects, and to compression problems resulting from the long bunch lengths in the damping rings. Thus, the SLC Linac can provide acceptable emittances at least to intensities of order $1 \times 10^{10} e^-$ at present.

Beam Energy and Energy Spectrum

The energies and energy spectra of the electron and positron bunches at the end of the SLC linac must be kept stable to approximately 0.1% and 0.2%, respectively, to transport the bunches through the Arc and Final Focus systems efficiently so that a small collision spot can be made.² The energy is measured after the Arc beam splitter magnet using a beam position monitor at a location with a design dispersion of 70 mm. Position monitors before the bend are used to remove trajectory errors from the energy errors. The energy can be measured on every pulse and the jitter studied^{2,4}. Typical rms energy jitter without feedback is 0.1 to 0.2%. A summary of the energy faults is shown in Table II. The faults which are outside three sigma of the mean and could not be fixed by a ten pulse average feedback system are included. The percentage of pulses which would provide low luminosity is 7.4%, 3.5% for only RF-related issues.

Table II

Missing energy pulses per 10000 beam pulses.
One hour sample at 5 pps, 47 GeV.

Missing Trigger	25
Klystron Cycles	50
Energy Offsets (Steps)	100
Single Klystron Faults	160
Low Beam Current	350
Sub-Booster Trip	50
Total	735

The energy spectra are measured using synchrotron radiation generated in vertical wiggler magnets and viewed on non-intercepting X-ray sensitive screens viewed by TV cameras⁹. Energy spectra measurements have been obtained as a function of current². Typical measured widths are in the range 0.2 to 0.5 percent. However, unexpected transverse position-energy correlations before the splitter magnet have been shown to mix with the measurement of the energy spectrum and alter the results. Techniques to measure this correlation are being developed. One indication of the magnitude of this apparent dispersion is the position shifts at the end of the linac produced by upstream energy changes. Sub-boosters which drive eight

klystrons (~ 1.8 GeV) were added and subtracted from the beam, and the trajectory changes were recorded. The measured dispersion or $\Delta x/(\Delta E/E)$ as a function of location of the sub-booster is shown in Fig. 8 and is larger the farther away the energy change occurred. This may be explained by the increasing number of trajectory displacements hidden in BPM-magnet calibration and survey errors as the distance increases. As a complication, there are also chromatic and RF deflection issues involved. In addition, the RTL is known to produce nonzero dispersion at the entrance to the linac (~ 5 cm). This can be fixed with optics changes.

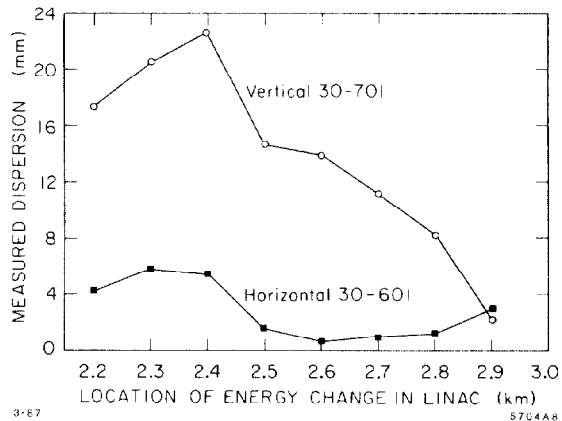


Fig. 8. Measured dispersion at the end of the linac as a function of location of the energy change.

The longitudinal wake potential has been measured by observing energy changes at the end of the linac as the intensity of the electron bunch is changed. A change in energy of 0.37 GeV was observed when the intensity was changed from 2.2×10^{10} to 8×10^9 . Taking into account bunch lengthening, the energy change was 90% higher than expected. This result is under investigation but does not impact the operation of the SLC.

Acknowledgments

Many people at SLAC have helped to make the commissioning of the SLC Linac proceed efficiently. Many thanks go to them all. Special thanks are extended to K. Bane, M. Ross, J. Sheppard, R. Stiening and the Operations Group. M. L. Arnold and Technical Illustrations kindly helped prepare this document.

References

1. J. Seeman and J. Sheppard, "Special SLC Linac Developments," 1986 Linac Conference, Stanford, 1986; also SLAC-PUB-3944.
2. G. Abrams et al., "Fast Energy and Energy Spectrum Feedback in the SLC Linac," 1987 Particle Accelerator Conference, Washington, D.C.
3. J. Seeman et al., "Transverse Wakefield Control and Feedback in the SLC Linac," 1987 Particle Accelerator Conference, Washington, D.C.
4. M. Allen et al., "Performance of the Stanford Linear Collider Klystrons at SLAC," 1987 Particle Accelerator Conference, Washington, D.C.
5. R. Jobe et al., "Position, Angle and Energy Stabilization for the SLC Positron Target and Arcs," 1987 Particle Accelerator Conference, Washington, D.C.
6. J. Sheppard et al., "Beam Steering in the SLC Linac," Particle Accelerator Conference, Vancouver, IEEE NS-32 No. 5, p. 2180, 1985.
7. J. Sheppard et al., "Commissioning of the SLC Injector," 1987 Particle Accelerator Conference, Washington, D.C.
8. M. Ross et al., "High Resolution Beam Profile Monitors in the SLC," 1985 Particle Accelerator Conference, IEEE NS-32 No. 5, p. 2003 (1985).
9. J. Seeman et al., "SLC Energy Spectrum Monitor using Synchrotron Radiation," 1986 Linac Conference, SLAC, p.441, (1986), also SLAC-PUB-3945.